Turkish Journal of Electrical Engineering & Computer Sciences

http://journals.tubitak.gov.tr/elektrik/

Research Article

Turk J Elec Eng & Comp Sci
(2015) 23: 1001 – 1008

doi:10.3906/elk-1304-150

A fourth-order accurate compact 2-D FDFD method for waveguide problems

Lokman KUZU*
R&D and Satellite Design Department, Gölbaşı, Ankara, Turkey

Received: 16.04.2013 • **Accepted/Published Online:** 30.06.2013 • **Printed:** 10.06.2015

Abstract: In this work, a fourth-order accurate 2-D finite difference frequency domain method is proposed for the analysis of general waveguide structures. Finite difference techniques have been extensively used to solve electromagnetic problems over the decades. These methods discretize the computational domain using the Yee cell, but the standard Yee scheme used in these methods is only second-order accurate. In order to demonstrate the advantages of the proposed scheme compared to the multiresolution frequency domain method and the traditional 2-D finite difference frequency domain scheme, the dispersion characteristics of various waveguide structures are analyzed.

Key words: Fourth-order 2-D finite difference frequency domain, multiresolution frequency domain, 2-D finite difference frequency domain, Yee cell, waveguides

1. Introduction

Finite difference methods have been successfully applied to waveguide problems in the past [1–9]. In all these works, either 2-D finite difference frequency domain (FDFD) or multiresolution frequency domain (MRFD) methods were employed. The 2-D FDFD scheme (FDFD(2)) relies on the approximation of space derivatives of Maxwell's curl equations by central differences on staggered grids, leading to a scheme that is only second-order accurate in space. This method requires significant amounts of computational resources for electrically large problems mainly due to the requirement of finer meshes compared to the grid size of higher order schemes. Although the space-stepping finite difference frequency domain (SSFDFD) method has been developed to overcome the requirement of large amounts of computer memory [10], it has stability issues because of the space stepping algorithm, similar to time stepping in FDFD. In order to solve such problems, higher-order 2-D FDFD schemes can be used. In this work, it has been shown that the fourth-order 2-D FDFD (FDFD(4)) method yields important computational savings in relation to the other methods without sacrificing solution accuracy. The approach given in this paper is mostly for metallic wall microwave waveguides. However, the 2-D FDFD(4) method is so versatile that even the anisotropic material can be solved easily by arranging the permittivity and permeability matrices accordingly.

2. FDFD(4) formulation

In finite difference methods, Maxwell's equations are discretized using a Yee cell [11] as shown in Figure 1. In this cell, location of the electric and magnetic field vectors are different and half-cell shifted. In each cell the electric field components are located at the centers of the edges of the cell, whereas the magnetic field

*Correspondence: lkuzu@turksat.com.tr

components are normal to the centers of the faces. There are no field components at the corners.

Due to this staggered fashion of the Yee cell, we use Taylor series of $f(x)$ expanded at half-grid points, which makes it easy to implement higher-order 2-D FDFD schemes for electromagnetic problems.

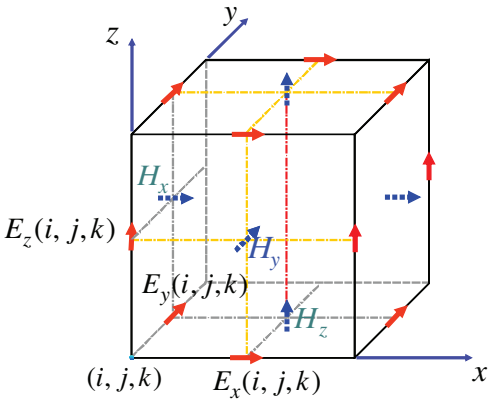

Figure 1. Three-dimensional Yee cell.

In order to develop the 2-D FDFD(4) scheme, one can take the Taylor series expansion of the function $f(x)$ at two sample points as follows.

$$f(x+h) = f(x) + h \cdot f'(x) + \frac{h^2}{2!} f''(x) + \frac{h^3}{3!} f'''(x) + \frac{h^4}{4!} f''''(x) + \frac{h^5}{5!} f^{(5)}(x) + \ldots \tag{1}$$

$$f(x+3h) = f(x) + 3h \cdot f'(x) + \frac{9h^2}{2!} f''(x) + \frac{27h^3}{3!} f'''(x) + \frac{81h^4}{4!} f''''(x) + \ldots \tag{2}$$

Similarly expand $f(x)$ at $x-h$ and $x-3h$ points. We multiply all these expansions with arbitrary numbers, such as c_1, c_2, c_3, and c_4. After regrouping similar terms and doing some manipulation, we obtain the following:

$$\begin{aligned} &c_1 f(x+h) + c_2 f(x-h) + c_3 f(x+3h) + c_4 f(x-3h) = (c_1 + c_2 + c_3 + c_4) f(x) \\ &+ h f'(x)(+c_1 - c_2 + 3c_3 - 3c_4) + \tfrac{h^2}{2!} f''(x)\,(c_1 + c_2 + 9c_3 + 9c_4) \\ &+ \tfrac{h^3}{3!} f'''(x)\,(+c_1 - c_2 + 27c_3 - 27c_4) + \max(c_1, c_2, c_3, c_4) \cdot O\left[h^4\right]. \end{aligned} \tag{3}$$

One can find c_1, c_2, c_3, and c_4 such that the linear combination of $c_1 f(x+h) + c_2 f(x-h) + c_3 f(x+3h) + c_4 f(x-3h)$ functions gives a good approximation of $f'(x)$ at point x. We impose the following conditions so that all other terms vanish and $f'(x)$ only remains.

$$\begin{aligned} c_1 + c_2 + c_3 + c_4 &= 0 \\ c_1 - c_2 + 3c_3 - 3c_4 &= \tfrac{1}{h} \\ c_1 + c_2 + 9c_3 + 9c_4 &= 0 \\ c_1 - c_2 + 27c_3 - 27c_4 &= 0 \end{aligned} \tag{4}$$

These equations can be written in matrix form as follows:

$$\begin{bmatrix} 1 & 1 & 1 & 1 \\ 1 & -1 & 3 & -3 \\ 1 & 1 & 9 & 9 \\ 1 & -1 & 27 & -27 \end{bmatrix} \begin{bmatrix} c_1 \\ c_2 \\ c_3 \\ c_4 \end{bmatrix} = \begin{bmatrix} 0 \\ \frac{1}{h} \\ 0 \\ 0 \end{bmatrix}. \tag{5}$$

Solving this linear system, we obtain:

$$c_1 = \frac{27}{48h},\ c_2 = \frac{-27}{48h},\ c_3 = \frac{-1}{48h},\ c_4 = \frac{1}{48h}, \tag{6}$$

where $h = \frac{\Delta x}{2}$ is the half of the grid size.

From here, one can obtain a fourth-order accurate 2-D FDFD scheme as follows:

$$\begin{aligned} f'(x) \quad = \quad & -\frac{1}{24\Delta x} f(x + \frac{3\Delta x}{2}) + \frac{27}{24\Delta x} f(x + \frac{\Delta x}{2}) - \frac{27}{24\Delta x} f(x - \frac{\Delta x}{2}) \\ & + \frac{1}{24\Delta x} f(x - \frac{3\Delta x}{2}) + O[(\Delta x)^4]. \end{aligned} \tag{7}$$

For the fourth-order scheme, the error term in the approximation of the derivative is of the form $O[(\Delta x)^4]$, and the number of the electromagnetic field nodes involved in the computation of each field component is increased with respect to the second-order scheme.

3. Waveguide structures

It is very important to analyze the waveguide structures accurately since they are used as port data for simulation of microwave devices. The 2-D FDFD(2) method consume too many computational resources when compared to other frequency domain methods such as the eigen-based multiresolution finite difference frequency domain method developed in [9]. These methods are used to analyze the characteristics of waveguides, such as propagation constant, mode patterns, and characteristic impedance.

3.1. 2-D formulation

Assuming that the waveguide structure is uniform along the z axis and the wave is propagating in the positive z direction, the electric and magnetic fields inside a waveguide can be expressed as:

$$\begin{aligned} \overrightarrow{E}(x,y,z) &= [E_x\hat{x} + E_y\hat{y} + E_z\hat{z}]\, e^{-j\beta z} \\ \overrightarrow{H}(x,y,z) &= [H_x\hat{x} + H_y\hat{y} + H_z\hat{z}]\, e^{-j\beta z} \end{aligned}, \tag{8}$$

where β is the propagation constant.

The differential Maxwell equations in the frequency domain for simple dielectric media are:

$$\begin{aligned} \nabla \times \overrightarrow{E} &= -j\omega\mu\overrightarrow{H} \\ \nabla \times \overrightarrow{H} &= j\omega\varepsilon\overrightarrow{E} \end{aligned}, \tag{9}$$

$$\begin{aligned} \nabla \bullet \overrightarrow{D} &= 0 \\ \nabla \bullet \overrightarrow{B} &= 0 \end{aligned}, \tag{10}$$

in which the space derivatives with respect to z can be replaced by $-j\beta$ (i.e. $\partial/\partial z = -j\beta$). Substituting Eq. (8) into the Maxwell curl equations of Eq. (9), the following scalar equations can be obtained.

$$\beta E_x(x,y) = \omega\mu_y H_y(x,y) + j\frac{\partial E_z(x,y)}{\partial x} \tag{11}$$

$$\beta E_y(x,y) = -\omega\mu_x H_x(x,y) + j\frac{\partial E_z(x,y)}{\partial y} \tag{12}$$

$$j\omega\varepsilon_z E_z(x,y) = \frac{\partial H_y(x,y)}{\partial x} - \frac{\partial H_x(x,y)}{\partial y} \tag{13}$$

$$\beta H_x(x,y) = -\omega\varepsilon_y E_y(x,y) + j\frac{\partial H_z(x,y)}{\partial x} \tag{14}$$

$$\beta H_y(x,y) = \omega\varepsilon_x E_x(x,y) + j\frac{\partial H_z(x,y)}{\partial y} \tag{15}$$

$$j\omega\mu_z H_z(x,y) = -\frac{\partial E_y(x,y)}{\partial x} + \frac{\partial E_x(x,y)}{\partial y} \tag{16}$$

Since Eqs. (13) and (16) don't include β, we cannot calculate the propagation constant using four equations with six unknowns. Therefore, two additional equations can be obtained by substituting Eq. (8) into Eq. (10) as follows.

$$\beta\varepsilon_z E_z(x,y) = -j\varepsilon_x\frac{\partial E_x(x,y)}{\partial x} - j\varepsilon_y\frac{\partial E_y(x,y)}{\partial y} \tag{17}$$

$$\beta\mu_z H_z(x,y) = -j\mu_x\frac{\partial H_x(x,y)}{\partial x} - j\mu_y\frac{\partial H_y(x,y)}{\partial y} \tag{18}$$

The fourth-order accurate 2-D finite difference scheme given in Eq. (7) can be applied to the six scalar equations in Eqs. (11) though (18) to solve waveguide problems. To do this, compact 2-D Yee cells are used to discretize the equations. The cell structure is obtained simply by collapsing the 3-D Yee cell in the z direction. Only the first three of the resulting update equations are presented here as an example. The remaining update equations, which are not listed here due to space considerations, can be derived similarly by applying the same procedure. For Eq. (11), the grid structure is shown in Figure 2.

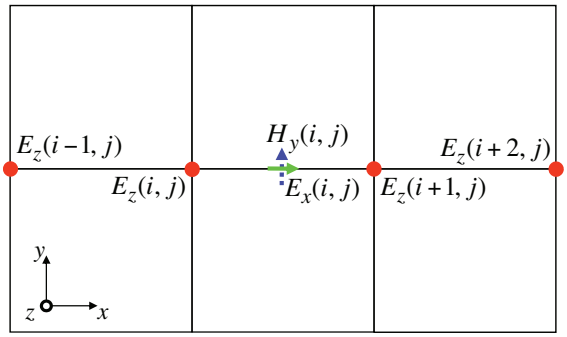

Figure 2. 2-D compact Yee cell.

$$\beta \mathrm{E}_x(i,j) = \omega\mu_y(i,j)H_y(i,j) + \frac{j}{24\Delta x}\begin{bmatrix} -E_z(i+2,j) \\ +27E_z(i+1,j) \\ -27E_z(i,j) \\ +E_z(i-1,j) \end{bmatrix} \tag{19}$$

$$\beta E_y(i,j) = -\omega\mu_x H_x(i,j) + \frac{j}{24\Delta y}\begin{bmatrix} -E_z(i,j+2) \\ +27E_z(i,j+1) \\ -27E_z(i,j) \\ +E_z(i,j-1) \end{bmatrix} \tag{20}$$

$$\begin{aligned} \beta \mathrm{E}_z(i,j) = {} & \tfrac{-j}{\varepsilon_z(i,j)}\tfrac{1}{2}\begin{bmatrix} \varepsilon_x(i,j) \\ +\varepsilon_x(i-1,j) \end{bmatrix}\tfrac{1}{24\Delta x}\begin{bmatrix} -E_x(i+1,j) \\ +27E_x(i,j) \\ -27E_x(i-1,j) \\ +E_x(i-2,j) \end{bmatrix} \\ & -\tfrac{j}{\varepsilon_z(i,j)}\tfrac{1}{2}\begin{bmatrix} \varepsilon_y(i,j) \\ +\varepsilon_y(i,j-1) \end{bmatrix}\tfrac{1}{24\Delta y}\begin{bmatrix} -E_y(i,j+1) \\ +27E_y(i,j) \\ -27E_y(i,j-1) \\ +E_y(i,j-2) \end{bmatrix} \end{aligned} \tag{21}$$

3.2. Treatment of the boundaries

The fields on the boundary must be computed with special boundary conditions. The tangential electric and normal magnetic fields are equal to zero at the PEC boundary. However, update equations written for the grid nodes in the vicinity of the boundary include the field components outside of the computational domain. The image principle is adopted to calculate those nodes [12]. Moreover, the continuity condition of electric fields across two dielectric mediums is established by taking the average of the dielectric constants in the two regions on the interface. In the 1-D Yee grid shown in Figure 3, for example, the following equations are used for the electric and magnetic field nodes outside of the computational domain. $E_y(i-1) = -E_y(i+1)$ and $H_y(i-1) = H_y(i)$.

After implementing all the boundary conditions, field update equations can be used to form an eigenvalue problem as follows:

$$[A] \cdot x = \beta\,[I] \cdot x, \tag{22}$$

where $[A]$ is a highly sparse matrix, $[I]$ is the identity matrix, and x is the unknown field vector. The eigensolution of $[A]$ delivers the propagation constant and eigenvectors of $[A]$ deliver the corresponding mode patterns.

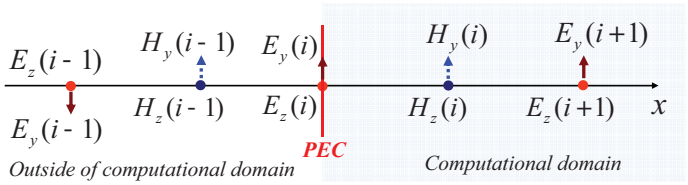

Figure 3. One-dimensional Yee grid and field components.

4. Numerical examples

In this section some numerical results are provided to illustrate the efficiency of the proposed method. All examples are coded in MATLAB and executed on a laptop PC equipped with 1.9 GHz processor and 2 GB RAM. Simulation results are compared to analytical calculations wherever possible [13].

4.1. Air-filled waveguide

First, we start with the result of an air-filled rectangular waveguide with dimensions $a = 1.5$ cm, $b = 0.6$ cm as illustrated in Figure 4. We assume that the waveguide is uniform along the z axis and the wave is propagating in the positive z direction. The propagation constants of the first-order mode are computed using FDFD(2), MRFD, and FDFD(4) methods. Results are compared to the analytical calculations in Figure 5.

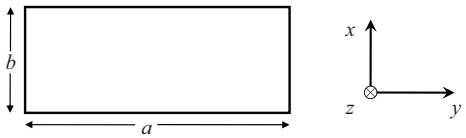

Figure 4. Air-filled waveguide.

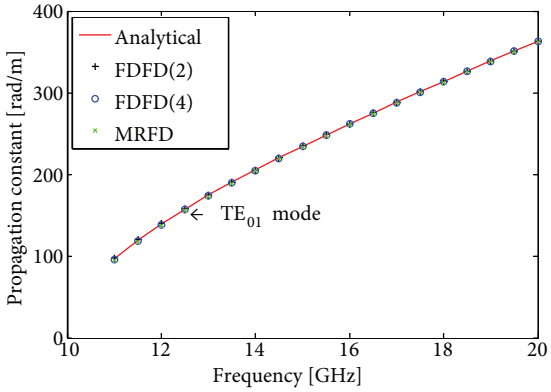

Figure 5. Propagation constant of the first propagating mode of an air-filled waveguide.

4.2. Partially filled waveguide

The second example is the same waveguide partially filled with a dielectric as shown in Figure 6. The relative dielectric constant of the substrate is $\varepsilon_r = 2.25$ and height is $h = 0.3$ cm. Computed propagation constant values are given in Figure 7. Taking the analytical value of propagation constant (β) at 10 GHz as a reference, computational errors of each method for different cell sizes are plotted in Figure 8. As the cell size becomes smaller, the FDFD(2) method converges reasonably fast. MRFD and FDFD(4) results are too close to differentiate at this scale.

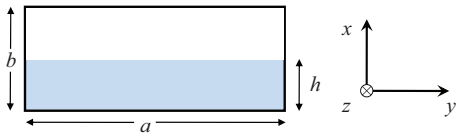

Figure 6. Partially filled waveguide.

4.3. Microstrip line

Finally, the propagation characteristics of the boxed microstrip line depicted in Figure 9 are considered. The dimensions are $a = 1.5$ cm, $b = 0.6$ cm, $h = 0.3$ cm, and $w = 0.3$ cm. Relative permittivity of the substrate (ε_r) is 30. The computed effective dielectric constant of this structure is shown in Figure 10.

For all three cases, the MRFD and FDFD(4) grids were chosen to be coarser than the standard FDFD grid, yet the accuracy of both methods remained identical to that of FDFD(2). Coarser mesh results in smaller matrix sizes and reduced computation time and memory requirements. For each example, cell size, simulation time, and matrix fill ratio are summarized in the Table below. Although FDFD(2) uses fewer nonzero elements in the matrix, the other techniques are faster because the matrix created by the FDFD(2) method is larger than

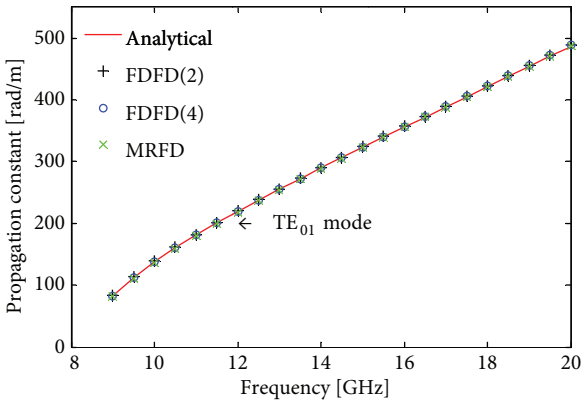

Figure 7. Propagation constant of the first propagating mode of a partially filled waveguide.

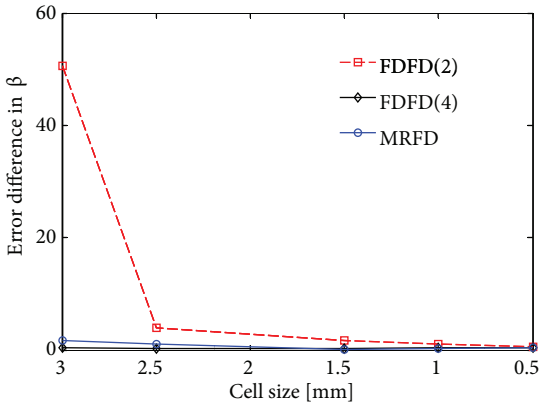

Figure 8. Error convergence of the propagation constant for each method.

the matrices created by other methods. Results show that the accuracy of the FDFD(4) method matches that of the FDFD(2) and MRFD methods despite savings in terms of memory and execution time.

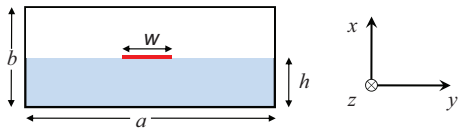

Figure 9. Microstrip line.

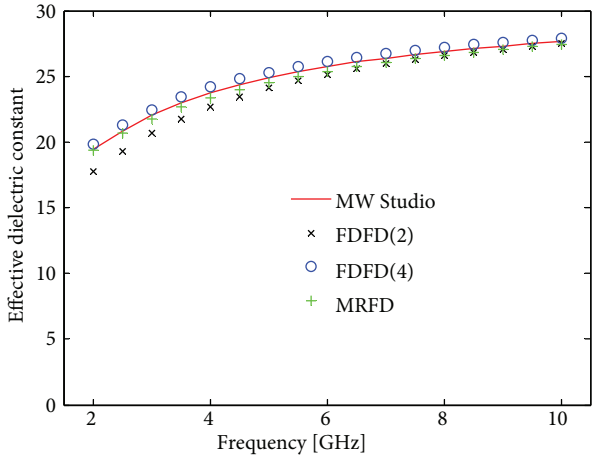

Figure 10. Effective dielectric constant of the boxed microstrip line.

Table. Comparison of simulation parameters.

		Mesh size	Sim. time (s)	Matrix fill ratio (%)
Air-filled rectangular Waveguide	FDFD(2)	15 × 6	14.49	0.6626
	FDFD(4)	5 × 4	6.86	5.0702
	MRFD	5 × 4	6.97	6.3377
Partially filled Waveguide	FDFD(2)	15 × 6	15.54	0.6626
	FDFD(4)	5 × 4	8.47	5.0702
	MRFD	5 × 4	8.61	6.3377
Microstrip line	FDFD(2)	15 × 6	6.79	0.6626
	FDFD(4)	10 × 4	4.94	2.4595
	MRFD	10 × 4	5.71	3.2373

5. Conclusion

In this paper, a fourth-order accurate FDFD scheme is developed and used to analyze the propagation characteristics of general waveguide structures. In order to show the effectiveness of the proposed method, numerical examples are provided and results are compared to MRFD and FDFD(2) schemes. Numerical results show that the FDFD(4) method achieves significant savings in terms of execution time and memory requirements.

References

[1] Xiao S, Vahldieck R, Jin H. Full-wave analysis of guided wave structures using a novel 2-D FDTD. IEEE Microw Guided W 1992; 2: 165–167.

[2] Asi A, Shafai L. Dispersion analysis of anisotropic inhomogeneous waveguides using compact 2D-FDTD. Electron Lett 1992; 28: 1451–1452.

[3] Cangellaris AC. Numerical stability and numerical dispersion of a compact 2-D/FDTD method used for the dispersion analysis of waveguides. IEEE Microw Guided W 1993; 3: 3–5.

[4] Lui ML, Chen Z. A direct computation of propagation constant using compact 2-D full-wave eigen-based finite-difference frequency-domain technique. In: International Conference on Computational Electromagnetics and its Applications; 1999; Beijing, China. pp. 78–81.

[5] Zhao YJ, Wu KL, Cheng KKM. A compact 2-D full-wave finite difference frequency-domain method for general guided wave structures. IEEE T Microw Theory 2002; 50: 1844–1848.

[6] Li LY, Mao JF. An improved compact 2-D finite-difference frequency domain method for guided wave structures. IEEE Microw Wirel Co 2003; 13: 520–522.

[7] Wang BZ, Wang X, Shao W. 2D full-wave finite-difference frequency domain method for lossy metal waveguide. Microw Opt Techn Let 2004; 42: 158–161.

[8] Pereda, JA, Vegas A, Velarde LF, Gonzalez O. An FDFD eigenvalue formulation for computing port solutions in FDTD simulators. Microw Opt Techn Let 2005; 45; 1–3.

[9] Gokten M, Elsherbeni AZ, Arvas E. The multiresolution frequency domain method for general guided wave structures. Prog Electromagn Res 2007; 69: 55–66.

[10] Mao J, Jiang L, Luo L. A novel space-stepping finite-difference frequency-domain method for full wave electromagnetic field modeling of passive microwave devices. Appl Comput Electrom 2009; 24: 259–267.

[11] Yee KS. Numerical solution of initial boundary value problems involving Maxwell's equations in isotropic media. IEEE T Antenn Propag 1966; 14: 302–307.

[12] Krumpholz M, Katehi LPB. MRTD: New time-domain schemes based on multiresolution analysis. IEEE T Microw Theory 1996; 44: 555–571.

[13] Harrington RF. Time-Harmonic Electromagnetic Fields. York, PA, USA: McGraw-Hill Book Company; 1961.